Nonequilibrium spectral diffusion due to laser heating in stimulated photon echo spectroscopy of low temperature glasses

Peter Neu*, Robert J. Silbey*, Stephan J. Zilker†, and Dietrich Haarer†

*Department of Chemistry and Center for Materials Science and Engineering, Massachusetts Institute of Technology, Cambridge, Ma. 02139

†Physikalisches Institut und Bayreuther Institut für Makromolekülforschung, Universität Bayreuth, D-95440 Bayreuth, Germany

(Submitted to PRB)

Abstract

A quantitative theory is developed, which accounts for heating artifacts in three-pulse photon echo (3PE) experiments. The heat diffusion equation is solved and the average value of the temperature in the focal volume of the laser is determined as a function of the 3PE waiting time. This temperature is used in the framework of nonequilibrium spectral diffusion theory to calculate the effective homogeneous linewidth of an ensemble of probe molecules embedded in an amorphous host. The theory fits recently observed plateaus and bumps without introducing a gap in the distribution function of flip rates of the two-level systems or any other major modification of the standard tunneling model.

I. INTRODUCTION

Glasses are commonly considered as nonequilibrated, structurally disordered solids. The amorphous network performs configurational fluctuations on a wide range of time scales. At low temperatures, tunneling through conformational barriers is assumed to be the dominant

relaxation mechanism. This view is equivalent to the two-level system (TLS) model[1,2] that has successfully accounted for many of the anomalous low-temperature properties of glasses.[3] In the standard formulation, it is assumed that TLS have on a logarithmic time scale a broad distribution of energy splittings, E, and relaxation rates, R,

$$P(E,R)\,dE\,d\log R \;\sim\; \text{constant} \;\times\; dE\,d\log R. \tag{1}$$

As a consequence, the observed relaxation dynamics in glasses depends on the experimental time scale. This has far-reaching implications for the linewidth of an optical transition of a probe molecule embedded in a glassy host: its transition frequency becomes a dynamical quantity.[4] This phenomenon is commonly referred to as spectral diffusion (SD). It prevents a definition of a homogeneous linewidth as in crystalline materials.

In an optical experiment, the absorption spectrum of an ensemble of chromophores doped into an amorphous host is measured. Due to inhomogeneities in the local strain or electric fields experienced by individual chromophores, this spectrum (the so-called inhomogeneous line) is several orders of magnitude broader than the linewidth of a single molecule. Hence, to monitor the local structural glass dynamics, line-narrowing techniques like two-, three-pulse (stimulated) photon echoes (2(3)PE) and hole burning (HB) have to be used.[5–8] Being conceptionally similar, the main difference of these techniques is the sensitivity to relaxation processes on different time scales: fast dephasing processes (pico–nanoseconds) caused by rapid TLS flips and vibrations of individual chromophores[9] are measured in 2PE; linewidths measured in 3PE (nano–milliseconds) and HB (microseconds–several days) are additionally broadened due to SD. The rates of SD may vary over many orders of magnitude. By convention, the linewidth measured in a 2PE experiment is called homogeneous. In the standard model, Eq. (1), a linear increase with temperature is predicted. The linewidth measured in 3PE and HB experiments is commonly referred to as "effective" homogeneous linewidth. According to Eq. (1), this line also broadens linearly with temperature. By the same token, SD induces a logarithmic broadening as a function of the waiting time (time between the second and third pulse in a 3PE, or between burning and reading a hole in a

HB experiment).[10–13]

Very recently, there has been broad interest in 3PE of Wiersma's group[15(a)–(e)], which—contrary to the standard model—showed a plateau between 10^{-6} and 10^{-3} s. They investigated the chromophore zincporphine in deuterated ethanol glass (ZnP/EtOD). Meijers and Wiersma interpreted their data by postulating a gap in the distribution of TLS rates in the microsecond region.[15(b)–(e)] Zimdars and Fayer emphasized, shortly after that, the contradiction between hole burning data of Fayer's group[7] and the 3PE data of Wiersma's group.[15(b)–(e)] To explain this difference, they invented a model, which is based on the assumptions that (1) the coupling between the chromophores and the glass can vary as a function of the TLS relaxation rates, and (2) TLS with relaxation rates in the microsecond domain couple to the chromophores only via an electric dipolar interaction. According to this, non-polar chromophores such as those used in Wiersma's experiment will not sense a perturbation by those electric TLS resulting in a gap in the relaxation rate distribution. The relevance of this model has been discussed by Silbey and co-workers.[16(b)] The same authors could fit Meijers' data qualitatively without assuming a gap, but starting out from a modified distribution function, which predicts a slower-than-logarithmic line broadening in the microsecond region.[16(a)–(b)] Silbey's model is based on computer simulations of a Lennard-Jones model glass.[17] Finally, it was Zilker and Haarer who shed light into the discussion by showing in the first 3PE experiment *below* 1 K that the line broadening does not only level off in the microsecond region, but in fact decreases again after several hundred microseconds.[18] They investigated the chromophore zinc meso-tetraphenylporphine in polymethylmethacrylate (ZnTPP/PMMA), a polymer glass. As the authors pointed out, this reversibility indicates laser induced sample heating artifacts, which may also be responsible for the gap previously observed in Wiersma's group.

It is the content of this work to clarify this point by treating the laser induced heating effect in a quantitative way, and reanalyzing the 3PE data of Meijers and Zilker.

The paper is organized as follows: in Sec. II, we brievely describe the experimental apparatus used in Ref. 18 and give an estimation of the heating effects for EtOD and PMMA

using the details of Meijers' and Zilker's experiment; in Sec. III, we present a simple model for the time dependence of the temperature in the focal volume of the laser beam by solving the heat diffusion equation for appropriate boundary conditions; in Sec. IV, we calculate the optical linewidth in the framework of nonequilibrium spectral diffusion[24]; in Sec. V, we compare with Meijers' and Zilker's 3PE data, and, in Sec. VI, we conclude.

II. EXPERIMENTAL

A. Stimulated photon echoes

The stimulated photon echo measurements in Ref. 18 (see Fig. 1) were performed with a tunable dye laser (Coherent 702-1CD) synchronously pumped by a mode-locked argon-ion laser (Coherent Innova 200-10). The output pulses (6 ps width) are cavity-dumped and amplified in two dye cell amplifiers which use a two-stage design. Each chain is pumped by its own frequency-doubled nanosecond Nd:YAG laser (Spectron SL404G) at a repetition rate of 10 Hz. After each stage a saturable absorber is used to suppress amplified spontaneous emission. Two beams with equal intensities are obtained from the resulting 1 μJ pulse of the first amplifier by a beam splitter. Beam 2 is fixed in time, whereas beam 1 can be delayed via a motorized delay line (DL1). The third pulse can be electronically delayed by picking any pulse from the 76 MHz pulse train emitted from the dye laser. Synchronization between the dye and the YAG lasers is accomplished via the reference signal of the mode-locker electronics, which triggers a digital delay generator (Stanford Research Systems DG535). The latter controls the firing of the flash lamps and the Q-switches of the YAG lasers and is also used to trigger the cavity-dumper of the dye laser. This design allows us to create pulses which can be electronically delayed with respect to each other from 100 ns up to 100 ms. An optical delay line (DL3) is used to realize waiting times shorter than 7 ns. The optical density of the sample was about 1 at the wavelength of the study, 597 nm. The laser was focused on the sample to a spot size of approximately 100 μm; the pulse energy was

about 3 nJ. The good optical quality of the samples enabled us to perform measurements of stimulated photon echoes without using an optical upconversion scheme.[25] The signal is spatially filtered to block most of the scattered light, and separated from the excitation beams by diaphragms. Finally, it is detected by a photomultiplier tube and registered with a boxcar integrator. The echo intensity depends nonlinearly on the energies of the excitation pulses. This makes an A/B–measurement for compensation of excitation energy fluctuations impossible. Therefore only data points, for which the energy of each laser pulse—measured by the two photodiodes (D)—is within a ±10 % window, are processed by the computer. Several scans of the delay line were averaged for each signal curve.

Zinc meso-tetraphenylporphine (ZnTPP, Porphyrin Products Inc.) was dissolved at a concentration of 1.5×10^{-4} M in the monomer methylmethacrylate; the polymerization of the mixture was initiated at 50° C. The resulting samples had a thickness of 1 mm and a radius of 4 mm. The fluorescence lifetime T_1 of ZnTPP in PMMA was measured as 7.5 ns in a transient-grating experiment.[26]

The sample was mounted in a ^{3}He bath cryostat (Janis Research Co.) providing a temperature range from 0.4 up to 4.0 K. The temperature was measured with a calibrated Germanium resistor (Lake Shore GR-200A-100) attached to the copper sample holder. Temperature control was achieved with an accuracy of ±0.01 K by heating the internal charcoal pump of the cryostat.

B. Heating effects in PMMA and EtOD

Let us assume that at $t = 0$ the total sample is in equilibrium with the helium bath at a temperature T_0 and illuminated by the (first and the second) laser beam. The laser irradiation excites via $S_0 \rightarrow S_1$ transitions those chromophores of the sample which are in its focal volume $V_{\mathrm{focal}} = \pi a^2 L_p$. The latter is a cylinder given by the spot size $a \approx 50\,\mu$m and the penetration depth $L_p \approx 0.5$ mm of the laser beam. The sample is cylindrically shaped with a radius R_0 of 4 mm and thickness $L = 1$ mm. The chromophores are assumed to be

homogeneously distributed in the illuminated volume, and the laser beam propagation is taken to be perpendicular to the circular surface of the sample. The excited chromophores irradiate heat, Q, over the fluorescence lifetime $\tau_{fl} \approx 1 - 10$ ns (in PMMA: $\tau_{fl} \approx 7.5$ ns, in EtOD: $\tau_{fl} \approx 2.7$ ns) due to intersystem crossings, $S_1 \rightarrow T$, to the triplet state. Since metalporphines such as ZnP and ZnTPP undergo these transitions with probabilities of more than 90 % ISC yield, up to 25 % of the incident laser energy can be transformed into heat during this process. If the heat release is considerably faster than the heat diffusion process out of the focal volume, we can assume that after a time τ_{fl} the chromophores have heated up the entire focal volume to a maximum temperature T_1 which is determined by the relation

$$Q = \int_{T_0}^{T_1} c(T) dT. \tag{2}$$

In PMMA, the specific heat is given by[19] $c(T) = 4.6\,T\,\mu\mathrm{J/gK}^2 + 29.2\,T^3\,\mu\mathrm{J/gK}^4$. Under the conditions of Zilker's 3PE experiment[18] (pulse energy of 3 nJ, ISC yield of 97 %, $\Delta E(\mathrm{singulet} - \mathrm{triplet}) = 3800\ \mathrm{cm}^{-1}$) for ZnTPP/PMMA, $Q = 20\ \mu$J/g is released into the sample which results in a local temperature increase inside the focal volume of $\Delta T = T_1 - T_0 \approx 0.55$ K for $T_0 = 0.75$ K. At $T_0 = 1.5$ K the heating effects amounts into $\Delta T \sim 0.2$ K, and no heating effect is expected at 3 K.

In EtOD glass, the specific heat is not known below 2 K. The value at two 2 K is roughly by a factor two larger than in PMMA: $c_{\mathrm{EtOD}}(2\,\mathrm{K}) \approx 350\ \mu\mathrm{J/gK}$.[21] The chromophore used in Meijers' experiment, ZnP, has very similar optical properties as ZnTPP, which was used in Zilker's experiment: ISC yield of 98 %, $\Delta E(\mathrm{singulet} - \mathrm{triplet}) = 3700\ \mathrm{cm}^{-1}$.[20] The applied pulse intensity in the 3PE experiment of Meijers and Wiersma has been quoted to be "less than 200 nJ per pulse" in Ref. 15(a) and "less than 100 nJ per pulse" in Ref. 15(d). Our estimation of the heating temperature, T_1, is based on a pulse intensity of 100 nJ/pulse. Since the optical properties of both chromophores are nearly identical, one can estimate the heat release into the sample in Meijers' experiment by multiplying Zilker's result by 100/3, which amounts in $Q \sim 650\ \mu$J/g. In PMMA, this provides a temperature increase of

$\Delta T \approx 1.6$, 0.8, and 0.6 K at $T_0 = 1.75$, 2.4, and 3 K, respectively. Since the specific heat in EtOD is roughly by a factor 2 larger than in PMMA, one has to divide these numbers by 2, yielding $T_1 \approx 2.55$, 2.8, and 3.3 K at $T_0 \approx 1.75$, 2.4, and 3 K, respectively.

III. HEAT DIFFUSION

Our goal is to determine the heat flow out of the focal volume by solving the heat diffusion equation

$$\frac{\partial}{\partial t} T(\mathbf{r}, t) - D \nabla^2 T(\mathbf{r}, t) = 0 \tag{3}$$

for the local temperature $T(\mathbf{r}, t)$, where the diffusion constant

$$D = \frac{\kappa}{\rho c} \tag{4}$$

is controlled by the heat conductivity κ, the mass density ρ, and the specific heat c of the sample. To calculate the line broadening, the spatially averaged temperature $T(t) = \langle T(\mathbf{r}, t) \rangle_{\mathbf{r} \in V_{\rm focal}}$ will be, eventually, plugged in the formalism of nonequilibrium spectral diffusion. The underlying assumption is that the phonons are in quasi-thermal equilibrium with the momentary temperature $T(t)$ in the focal volume, i.e., the TLS relaxation rates $R(T)$ are given by $R[T(t)]$. This is reasonable, because the phonon relaxation time is much shorter than the diffusion times (5)—(7). The replacement $T(r, t) \to T(t)$ is clearly approximate. In a correct treatment, the r dependence of the temperature has to be handled on the same footing as the r dependence of the dipole-dipole interaction ($\sim r^{-3}$) between the chromophore and the TLS in the host, which would, however, render the model too complicated.

There are three time scales for the heat diffusion process: the radial and longitudinal diffusion time over the time scales

$$\tau_a = a^2/D, \tag{5}$$

$$\tau_L = L_p^2/D, \tag{6}$$

and the time scale over which heat radiates into the helium bath [note $c(\mathrm{He}) \gg c(\mathrm{PMMA/EtOD})$]

$$\tau_r = R_K \rho c V_{\mathrm{focal}}, \tag{7}$$

which is controlled by the Kapitza surface resistance between a solid and liquid helium

$$R_K = \frac{0.05}{\pi a^2 T^3} \left[\frac{\mathrm{K^4 m^2}}{\mathrm{W}}\right]. \tag{8}$$

Although κ and c depend on temperature, we will assume in the following that D is temperature independent. Orders of magnitude for τ_a, τ_L, τ_r are given for PMMA in Table I.

Stimulated echo experiments are performed on the time scale between 0.1–1 ns to 10–100 ms. The plateau or the bump appears in the data between about 10 μs and 100 μs. This suggests the following picture: For $t < \tau_r \sim 2$ ms heat cannot radiate into the helium bath due to the large value of the boundary resistance R_K. Accordingly, the probe itself operates as a heat bath and absorbs the heat flow out of the focal volume in direction radial to the laser beam. At $\tau_L \gg \tau_a$ any inhomogeneous illumination of the focal volume in longitudinal direction becomes unimportant. The radial flow sets the time scale for equilibration with the helium bath after about $10 - 100$ μs. At this time scale, we would expect a bump in the stimulated echo data. After several hundred microseconds, we further expect a return to equilibrium spectral diffusion at $T = T_0$. Triplet heating can be excluded, since τ_r is much less than the time period between two consecutive echo pulse series (~ 75 ms). Both experiments confirm this picture (cf. Fig. 2 and 3).

Let us now perform our analysis more quantitatively. To solve the diffusion equation, appropriate boundary conditions have to be posed. First, to keep the model simple we neglect any heat conduction in propagation of the beam. This might be a crude approximation, however being justified by $\tau_a \ll \tau_r$ and because the laser beam penetrates almost the whole sample (penetration length $L_p \sim 0.5$ mm). The heat conduction in direction radial to the beam is governed by diffusion into the sample. Hence, we have to solve the diffusion

problem in an infinite (boundary effects due to a finite $R_0 = 4$ mm are not important in this experiment) cylindrical medium in which heat is produced by point sources (chromophores) at a rate $\sim \Delta Q(r) e^{-t/\tau_{fl}}$ ($r = \sqrt{x^2 + y^2}$). The amount of heat, $\Delta Q(r)$, released by the chromophore at position r is governed by the laser intensity, $I(r)$, at that point in the sample. We assume that the intensity profile across the diameter of the laser beam is Gaussian,

$$I(r) = P \frac{e^{-r^2/2a^2}}{2\pi a^2}, \tag{9}$$

where P is the total amount of beam power (in W) used. The exact solution to this problem is very complicated and beyond the scope of this paper. Instead we will treat a heat diffusion problem, which is equivalent in all physical aspects to the problem mentioned above. We assume that the chromophores have heated the focal volume to a higher temperature T_1 after the time τ_{fl}. If $\tau_{fl} \ll \tau_a$, the temperature profile is then well approximated by the laser intensity profile,

$$\Delta T(r, 0) = 2\Delta T \, e^{-r^2/2a^2}. \tag{10}$$

The normalization, we have chosen, is such that the average temperature in the focal volume at $t = 0$ is ΔT, i.e., $\Delta T = \int_0^\infty dr \, 2\pi r \Delta T(r, 0) \, e^{-r^2/2a^2}/2\pi a^2$. The temperature at a later time, t, is given by integration over the heat kernel[23]

$$\Delta T(r, t) = \frac{1}{4\pi D t} \int_{-\infty}^{\infty} dx' \int_{-\infty}^{\infty} dy' \, \Delta T(x', y', 0) \, e^{-[(x-x')^2 + (y-y')^2]/4Dt} = 2\Delta T \frac{e^{-r^2/2[\sigma(t)]^2}}{[\sigma(t)]^2/a^2}, \tag{11}$$

where

$$\sigma(t) = \sqrt{2Dt + a^2}. \tag{12}$$

Hence the average temperature $\Delta T(t) = \int_0^\infty dr \, 2\pi r \Delta T(r, t) \, e^{-r^2/2a^2}/2\pi a^2$ at a later time, t, reads

$$\Delta T(t) = \frac{\Delta T}{1 + t/\tau_a}. \tag{13}$$

Eventually, to account for the delay of the heat release over the time scale τ_{fl}, we subtract $e^{-t/\tau_{fl}}$ from Eq. (13). This corresponds to assuming that heat is produced at the rate

$(Q\rho/\tau_{fl})e^{-t/\tau_{fl}}$ per unit time and unit volume yielding a final temperature increase[23] $\Delta T = Q/c$. This, finally, gives

$$T(t) = T_0 + (T_1 - T_0)\left\{\frac{1}{1+t/\tau_a} \; - \; e^{-t/\tau_{fl}}\right\}. \tag{14}$$

Of course, this equation is only an approximation for the real solution of the diffusion problem posed above. As a consequence, the numerical value for ΔT and τ_a obtained from the fits by using (14) have to be seen as an order of magnitude estimation. However, our model contains all physical characteristics: (i) heat is supplied over the time scale τ_{fl} with an exponential rate, (ii) the temperature returns algebraically (non-exponentially) to equilibrium after the time scale τ_a. We have checked that (i) and (ii) are independent of the initial temperature profile (10). For instance $\Delta T(r,0) \propto \Theta(a-r)$ gives the same kind of behavior.

IV. OPTICAL LINEWIDTH

Hu and Walker[10] and Suarez and Silbey[13] have shown that three-pulse photon echo amplitude decays as $\exp[-\langle F_1(\tau) + F_2(\tau,t)\rangle_{\rm TLS}]$ due to TLS-flipping in the amorphous host. Here $\langle F_1(\tau)\rangle_{\rm TLS}$ is the two-pulse echo decay (or dephasing decay), and $\langle F_2(\tau,t)\rangle_{\rm TLS}$ is the decay that depends on the separation, t, between the second and the third pulse. $\langle ...\rangle_{\rm TLS}$ denotes the ensemble average over the TLS-relaxation rates, R, and the TLS-energy splittings, E. If τ lies well within a hyperbolic distribution of relaxation rates R, i.e., $R_{\rm min} \ll 1/\tau \ll R_{\rm max}$ and $P(R) \sim 1/R$, the effective, i.e., t depending dephasing rate $[1/T_2](t)$ is defined by $\langle F_1(\tau) + F_2(\tau,t)\rangle_{\rm TLS} = 2\tau/T_2(t)$. Analogously, the two-pulse echo decay rate, $1/T_{2,2\rm PE}$ is defined by $\langle F_1(\tau)\rangle_{\rm TLS} = 2\tau/T_{2,2\rm PE}$. Subtracting the lifetime contribution defines the pure dephasing rate $1/T^*_{2,2\rm PE} = 1/T_{2,2\rm PE} - 1/2T_1$. The effective homogeneous linewidth measured in a 3PE experiment is defined by

$$[1/\pi T_2^*](t) = [1/\pi T_2^*]_{2\rm PE} + [1/\pi T_2^*]_{\rm SD}(t) \tag{15}$$

where the last term, arising from $F_2(\tau,t)$, is the contribution due to spectral diffusion. For TLS and phonons in thermal equilibrium at temperature T_0 with a hyperbolic distribution

in TLS-relaxation rates, R, and a flat distribution in the TLS-energy splitting, E, (cf. Eq. (1)) one finds the well-known result

$$[1/\pi T_2^*](t) = KT_0\,[\,3.66\ +\ \log(R_{\rm eff}t)\,]\ +\ \Gamma_{\rm PLM}. \tag{16}$$

Here, K is a collection of constants proportional to the dipole-dipole interaction strength between the TLS and the chromophore, and $R_{\rm eff}$ is an effective relaxation rate averaged over the TLS splittings, E, (see below). The second term, $[1/\pi T_2^*]_{\rm SD}(t) \propto \log(R_{\rm eff}t)$, is the waiting time dependent contribution due to spectral diffusion. The first and the last term describe pure dephasing. At very low temperatures the term linear in T is dominant. This term arises from $F_1(\tau)$ and is characteristic for TLS-induced dephasing in amorphous solids. The last term, characterized by an activated temperature dependence

$$\Gamma_{\rm PLM} = b\,\frac{\exp(-\Delta E/k_BT)}{[1-\exp(-\Delta E/k_BT)]^2}, \tag{17}$$

also appears in molecular mixed crystals. It is a pure dephasing mechanism arising from vibrational modes of individual chromophores (pseudo-local phonon modes).[9] This mechanism usually starts to be dominant in the temperature regime between 1 and 3 K.

Recently, Silbey et al.[16(a)] have introduced a new model based on molecular dynamics simulations on a Lennard-Jones computer glass.[17] In the simulations for Ni-P at a given composition, it was found that the distribution function $P(\Delta)$ of the tunneling frequency, Δ, is hyperbolic for Δ/k_B less than $\sim 10^{-3}$ K, but as Δ increases, $P(\Delta)$ is best fitted by a form $1/\Delta^{1-\nu}$ where ν increases to ~ 0.2 as Δ/k_B increases beyond 1 K. With a typical maximum relaxation rate of about 10^{10} s^{-1} at 1 K, this implies that the standard model ($\nu = 0$) does not apply for waiting times shorter than $\sim 10^{-3} - 10^{-4}$ s. Although these results are not quantitatively accurate for all glasses, we will see that they provide a more reliable picture in the investigation of heating effects in the 3PE data below. The distribution function of TLS-relaxation rates and energy splittings is modified in this model according to

$$P(E,R) = \text{constant} \times \frac{E^\nu (R/R_{\rm max})^{\nu/2}}{R\sqrt{1-R/R_{\rm max}}}. \tag{18}$$

(We set Silbey's second parameter $\mu \equiv 0$.[16(a)]) This yields a two-pulse decay varying as $\exp[-(2\tau/T_{2,2\mathrm{PE}})^{1-\nu/2}]$, which is very close to an exponential decay for fits of experimental data. In the limit $\nu \ll 1$, the effective homogeneous linewidth is then found to behave like

$$[1/\pi T_2^*](t) = K_\nu T_0^{1+\nu} \left(\Theta_\nu \; + \; (2/\nu)[1 - (R_{\mathrm{eff}} t)^{-\nu/2}] \right) + \Gamma_{\mathrm{PLM}}, \tag{19}$$

where

$$R_{\mathrm{eff}}^{-\nu/2} = \frac{\int_0^{E_{\max}} dE\, E^\nu \,\mathrm{sech}^2(E/2k_BT)\, R_{\max}^{-\nu/2}}{\int_0^{E_{\max}} dE\, E^\nu \,\mathrm{sech}^2(E/2k_BT)}, \tag{20}$$

and (replacing $E_{\max}/2k_BT$ by infinity)

$$K_\nu = K \int_0^\infty dx\, x^\nu \mathrm{sech}^2(x) \tag{21}$$

with $\Theta_{\nu=0} = 3.66$ and $\Theta_{\nu=0.25} \approx 3.4$ (note $K_{\nu=0} = K$).

To calculate the spectral diffusion contribution in the case of heating over the time scale t, it is more convenient to use the formalism of Black and Halperin.[11] According to this, the contribution to the optical linewidth due to spectral diffusion is determined by the number of TLS, $n_f(t)$, which have flipped an odd number of times during the time t. Denoting the initial occupation of the upper (lower) state by $n_+(0)$ ($n_-(0)$), and the upwards (downwards) relaxation rate by W_+ (W_-), a simple master equation approach yields

$$n_f(t) = \frac{n_-(0)W_+ + n_+(0)W_-}{R}(1 - e^{-tR}), \tag{22}$$

where $R = W_+ + W_-$. In our case, all TLS are initially in thermal equilibrium with the helium heat bath at T_0. Hence, $n_+(0) = [\exp(E/k_BT_0) + 1]^{-1}$ and $n_-(0) = [1 + \exp(-E/k_BT_0)]^{-1}$. If we assume quasi-thermal equilibrium for the phonons, i.e., if we assume that the phonons are at the momentary temperature (14), the relaxation rates become time dependent and satisfy $W_+(t)/R(t) = [\exp(E/k_BT(t)) + 1]^{-1}$ and $W_-(t)/R(t) = [1 + \exp(-E/k_BT(t))]^{-1}$, with the one-phonon rate

$$R[r, T(t), x] = r R_{\max}[T(t), x], \tag{23}$$

$$R_{\max}[T(t), x] = c\, T_0^3 x^3 \coth[xT_0/T(t)], \tag{24}$$

where $x = E/2k_BT_0$ and $c \approx 10^{10}$ K^{-3} s^{-1}. In the experimentally relevant parameter regime, the exact numerical solution of the master equation with time dependent rates is very exactly described by the following analytical expression:

$$n_f(t) = (1/2)\{1 - \tanh[E/2k_BT_0]\tanh[E/k_BT(t)]\}\left(1 - e^{-tR[r,T(t),x]}\right). \tag{25}$$

The average of $n_f(t)$ over the TLS-energy splitting, E, and the dimensionless relaxation rate, $r \equiv R/R_{\max}$, is now performed using the distribution function (18). With this, the effective homogeneous linewidth at the momentary temperature $T(t)$ reads

$$[1/\pi T_2^*](t) = K_\nu T_0^{1+\nu}\,[\,\Theta_\nu + f_\nu(t, R_{\max}[T(t)])\,] + \Gamma_{\rm PLM}, \tag{26}$$

where

$$f_\nu(t, R_{\max}[T(t)]) = \frac{\int_0^\infty dx\,[1 - (t\,R_{\max}[T(t),x])^{-\nu/2}]\,[1 - \tanh(x)\tanh(xT_0/T(t))]}{(\nu/2)\int_0^\infty dx\;x^\nu\,\mathrm{sech}^2(x)}. \tag{27}$$

The result for the standard model arises in the limit $\nu \to 0$. In Fig. 2 and 3, $[1/\pi T_2^*](t)$ [(19) and (26)] is shown together with 3PE data of Ref. 15(d) for ZnP in EtOD, and Ref. 18 for ZnTPP in PMMA. In Fig. 4, 2PE data of ZnTPP and tetra-tert-butyl-terrylene (TBT) in PMMA are shown together with fits made with

$$[1/\pi T_2^*]_{\rm 2PE} = K_\nu\,T_0^{1+\nu}\Theta_\nu + \Gamma_{\rm PLM}. \tag{28}$$

V. COMPARISON TO EXPERIMENT

Meijers and Wiersma[15] have studied the 3PE decay of various chromophores in a number of different glasses. In order to fit their data they were forced to modify the standard model (1) by postulating the existence of a gap in the distribution of TLS flip rates on the time scale between micro- and milliseconds. For the system ZnP/EtOD, they assumed that the decay rate is linear in $\log(t)$ from the earliest times ($\sim 10^{-10}$ s) to 10^{-6} s, flat until 10^{-3} s, and then once more linear above 10^{-3} s, with the same slope as in the early time regime. As discussed in Ref. 16(a), the physical nature of this gap remains totally unclear.

Zilker and Haarer[18] have studied for the first time a 3PE decay below 1 K. They found at 0.75 K for the system ZnTPP/PMMA that the decay rate increases from the earliest times ($\sim 10^{-10}$ s) to 10^{-6} s, levels off, and *decreases* after ~ 300 μs. As the authors noted, this reversibility clearly indicates laser heating artifacts in the sample. Clearly, the question arises whether laser heating might also turn out to be responsible for the observation of a plateau in Meijers' and Wiersma's data.

In Ref. 16(a)-(b), Meijers' and Wiersma's data have been analyzed with the modified standard model using Eq. (19). The authors have found qualitative agreement with better quality fits emerging for the high temperature data. Zilker and Haarer[18] also analyzed successfully their data at 1.5 and 3 K, but not at 0.75 K, within this model.

In Fig. 2(a), we show the 3PE data for ZnP/EtOD at three temperatures, taken from the thesis of Meijers,[15(d)] with two fits using Eq. (19), dashed dotted line, and Eq. (26), full line. As noted already in Ref. 16, the need for a gap in the distribution function has disappeared. As shown in the figure, the predicted value of the 2PE decay rates also agree with experiment. One clearly sees from this plot, that including heating artifacts into the theoretical description improves the fits to the 1.75 and 2.4 K data, significantly. We have demonstrated this more clearly in Fig. 2(b). The initial temperature increase due to laser heating is $\Delta T = 0.9$, 0.4, and 0.3 K at $T_0 = 1.75$, 2.4, and 3 K, respectively. Both 3PE and 2PE show consistently that the contribution to pure dephasing of pseudo-localized librational modes of the guest chromophores in the amorphous matrix is insignificant even at 3 K for ZnP in EtOD glass.[15(c)]

In Fig. 3(a), the 3PE data for ZnTPP/PMMA taken from Zilker and Haarer[18] are plotted along with our theory in the same way. Again the data can be fitted with no gaps in the distribution function, and with parameter values close to those used in Figs. 2(a)-(b). The reversibility of the line broadening for the 0.75 K data is well reproduced by our theory, as depicted in Fig. 3(b). This clearly shows the influence of laser heating artifacts. No heating effect is observed at 3 K data; the temperature increase at 0.75 and 1.5 K is found to be 0.75 and 0.2 K, respectively. However, the predicted value of the 2PE decay rates is much lower

than the experimental value. The 3PE data for ZnTPP/PMMA can well be fitted without (or with only a small, cf. Fig. 4) contribution from localized phonon modes. Contrary to this, the 2PE data clearly show a deviation from a power law temperature dependence above ~ 2 K, which indicates active localized vibrations of the chromophores. In Fig. 4, we have illustrated this using recently published 2PE data for ZnTPP/PMMA[26] together with new results for TBT/PMMA. The full line shows a fit of Eq. (28) with $\nu = 0.18$. The best fit is obtained with $\nu = 0$ (dashed line). The dashed dotted line demonstrates the discrepancy between the experimental data and Eq. (28) when the parameter set obtained from the 3PE data (Fig. 3) is used. This may indicate that there are extra dephasing processes in these systems other than those described by the present model.

The parameters for the heating process are summarized in Table II. There is close agreement between the estimations for T_1 presented in Sec. II and the fit values. For PMMA, the fit value of the diffusion time τ_a is about one order of magnitude larger than the estimations in Table I. For pulse intensities less than 100 nJ in Meijers' and Wiersma's experiment the agreement between estimated (Eq. 2) and fitted value for T_1 is less close, although the discrepancies are insignificant given the uncertainties in the experimental parameters for EtOD.

It must be stressed that a fit to the 3PE data is also possible, if one uses the standard model with $\nu = 0$. However, the heating temperature we had to assume in this case were too high. Since $\nu \neq 0$ introduces already a weak bending of the decay rates, it also brings down the value for T_1 to realistic values. We consider this observation as an indication that it is necessary to change the standard model in the short time regime. For longer waiting times, $\gtrsim 10^{-3}$ s, the experiment explores that part of the distribution function, which becomes more and more hyperbolic. Hence, the bending of the decay rates should become weaker and, eventually, merge into the linear growth with $\log(t)$ usually observed in HB experiments. We believe that the deviation of the data from our theory in the millisecond regime indicates this transition.

VI. CONCLUSIONS

We have extended Silbey's modified standard model for dephasing and spectral diffusion in optical experiments to the situation of a nonequilibrated phonon bath. In particular, we have studied the situation in which the focal volume of a laser beam in an amorphous host is heated to some temperature T_1, and cools down to the temperature of the helium bath by heat diffusion. The resulting nonlogarithmic line broadening of chromophore molecules embedded in the glass due to spectral diffusion has been calculated. Our motivation has been to investigate whether this picture explains recently observed plateaus and bumps in 3PE data. We conclude that laser heating effects are important for 3PE experiments in the kelvin regime. This together with a modified, slightly bended equilibrium line broadening quantitatively accounts for the experimental data. However, since no studies of the 3PE decay on laser fluence are available up to now, the experimental evidence in favor of heating artifacts is indirect. A study of the fluence dependence remains an *essential* experiment to test the significance of heating effects.

ACKNOWLEDGMENTS

This research has been supported by the National Science Foundation, the Alexander von Humboldt Foundation, and the Deutsche Forschungsgemeinschaft, SFB279. We also thank Daan Thorn Lesson, David R. Reichman. Frank L. H. Brown, and Yu. G. Vainer for discussions.

REFERENCES

[1] W. A. Phillips, J. Low Temp. Phys. **7**, 351 (1972).

[2] P. W. Anderson, B. I. Halperin, and C. M. Varma, Philos. Mag. **25**, 1 (1972).

[3] For a review see: *Amorphous Solids—Low Temperature Properties*, Topics in Current Physics **24**, edited by W. A. Phillips (Springer, Berlin Heidelberg New York, 1984).

[4] J. Friedrich and D. Haarer, Angew. Chem. Int. Ed. Engl. **23**, 113 (1984).

[5] R. van den Berg and S. Völker, Chem. Phys. Lett. **137**, 201 (1987); R. van den Berg, A. Visser, and S. Völker, Chem. Phys. Lett. **144**, 105 (1988).

[6] Y. S. Bai and M. D. Fayer, Phys. Rev. B **39**, 11066 (1989).

[7] K. A. Littau and M. D. Fayer, Chem. Phys. Lett. **176**, 551 (1991).

[8] H. Maier, B. M. Kharlamov, and D. Haarer, Phys. Rev. Lett. **76**, 2085 (1996).

[9] B. Jackson and R. J. Silbey, Chem Phys. Lett. **99**, 331 (1983).

[10] P. Hu and L. R. Walker, Phys. Rev. B **18**, 1300 (1978).

[11] J. L. Black and B. I. Halperin, Phys. Rev. B **16**, 2879 (1977).

[12] T. L. Reinecke, Solid State Commun. **32**, 1103 (1979).

[13] R. J. Silbey and A. Suarez, Chem. Phys. Lett. **218**, 445 (1994).

[14] D. Zimdars and M. D. Fayer, J. Chem. Phys. **104**, 3865 (1996).

[15] (a) H. C. Meijers and D. A. Wiersma, Chem. Phys. Lett. **181**, 312 (1991); (b) Phys. Rev. Lett. **68**, 381 (1992); (c) J. Chem. Phys. **101**, 6927 (1994); (d) H. C. Meijers, Ph.D. thesis, U. Groningen, 1994; (e) D. Thorn Leeson and D. A. Wiersma, J. Phys. Chem. **98**, 3913 (1994).

[16] (a) R. J. Silbey, J. M. A. Koedijk, and S. Völker, J. Chem. Phys. **105**, 901 (1996); (b) J.

M. A. Koedijk, R. Wannemacher, R. J. Silbey, and S. Völker, J. Phys. Chem. **100**, 19945 (1996).

[17] A. Heuer and R. J. Silbey, Phys. Rev. Lett. **70**, 3911 (1993); Phys. Rev. B **49**, 1441 (1994); Phys. Rev. B **53**, 609 (1996).

[18] S. J. Zilker and D. Haarer, J. Chem. Phys. in print.

[19] R. B. Stephens, G. S. Cieloszyj, and G. L. Salinger, Phys. Lett. **38A**, 215 (1972).

[20] A. T. Gradyushko and M. P. Tsvirko, Opt. Spectr. **4**, 291 (1971).

[21] M.A. Ramos, Q.-W. Zou, S. Vieira, and F.J. Bermejo, Czech. J. Phys. **46**, 2235 (1996).

[22] A. Nittke, M. Scherl, P. Esquinazi, W. Lorenz, Junyun Li, and F. Pobell, J. Low Temp. Phys. **98**, 517 (1995).

[23] H. S. Carslaw, J. C. Jaeger, *Conduction of heat in Solids*, second edition, Oxford University Press, Oxford (1959).

[24] K. Fritsch, J. Friedrich, and B. M. Kharlamov, J. Chem. Phys. **105**, 1798 (1996).

[25] W. H. Hesselink and D. A. Wiersma, Chem. Phys. Lett. **56**, 227 (1978).

[26] S. J. Zilker and D. Haarer, J. Chem. Phys. **105**, 10648 (1996).

FIGURE CAPTIONS

FIG. 1: Experimental setup for stimulated photon echo measurements. "50/50" marks 50 % beam splitters, DL1–3 are optical delay lines, D photodiodes, and PMT is a photomultiplier tube.

FIG. 2: (a) 3PE decay rates, $[1/\pi T_2^*](t)$, as a function of the waiting time, t, for ZnP in EtOD, from Ref. 15. The lines are fits to the data: (—) heating effects included [Eq. (26)], $(- \cdot -)$ no heating effects included [Eq. (19)]. Effective relaxation rates used are $R_{\rm eff} = 1.2 \times 10^9 {\rm s}^{-1}$ ($\circ$), $R_{\rm eff} = 2.8 \times 10^9 {\rm s}^{-1}$ ($*$), $R_{\rm eff} = 3.5 \times 10^9 {\rm s}^{-1}$ ($\times$). The parameters for the heating process are $\tau_a = 15$ μs, $T_1 = 2.65$ K ($\circ$), $T_1 = 2.8$ K ($*$), and $T_1 = 3.3$ K ($\times$). The values of the 2PE decay rates are also given in the figure (+) along with the prediction of the model (dotted lines) with $K_\nu = 26.9$ MHz/K$^{1+\nu}$. The contribution of $\Gamma_{\rm PLM}$ is neglected in the fits at all three temperatures. (b) Same as (a) but only the data at $T_0 = 1.75$ K are shown.

FIG. 3: (a) 3PE decay rates, $[1/\pi T_2^*](t)$, as a function of the waiting time, t, for ZnTPP in PMMA, from Ref. 18. The lines are fits to the data: (—) heating effects included [Eq. (26)], $(- \cdot -)$ no heating effects included [Eq. (19)]. Effective relaxation rates used are $R_{\rm eff} = 10^{11} {\rm s}^{-1}$ ($\circ$), $R_{\rm eff} = 1.3 \times 10^{11} {\rm s}^{-1}$ ($*$), $R_{\rm eff} = 2.6 \times 10^{11} {\rm s}^{-1}$ ($\times$). The parameters for the heating process are $\tau_a = 300$ μs, $T_1 = 1.5$ K ($\circ$), $T_1 = 1.7$ K ($*$), and $T_1 = T_0$ ($\times$). The values of the 2PE decay rates are also given in the figure (+) along with the prediction of the model (dotted lines) with $K_\nu = 15.2$ MHz/K$^{1+\nu}$, $b = 0.9$ GHz, and $\Delta E = 9.7$ cm^{-1}. (b) Same as (a) but only the data at $T_0 = 0.75$ K are shown.

FIG. 4: 2PE decay rate, $[1/\pi T_2^*]_{\rm 2PE}$, for ZnTPP ($\circ$) and TBT ($*$) in PMMA. The solid line is a fit of Eq. (28) to the data for $\nu = 0.18$, $K_\nu = 24$ MHz/K$^{1+\nu}$, $b = 15.8$ GHz, and $\Delta E = 9.7$ cm^{-1}. The dashed line is a fit of Eq. (28) with $\nu = 0$, $K = 25.7$ MHz/K, $b = 12.7$ GHz, and $\Delta E = 8.8$ cm^{-1}. The dashed dotted line shows Eq. (28) with parameter values obtained from the fit to the 3PE data [Fig. 2(a)]: $\nu = 0.18$, $K_\nu =$

15.2 MHz/K$^{1+\nu}$, $b = 0.9$ GHz, and $\Delta E = 9.7$ cm^{-1}.

TABLE CAPTIONS

Table I: Diffusion times in PMMA with $\rho = 1.18$ g/cm^3, $c = 4.6\,T\,\mu$J/gK^2 + $29.2\,T^3\,\mu$J/gK^4 (Ref. 19), and $\kappa = (15, 20, 30, 42, 50) \times 10^{-3}$ W/mK (Ref. 22) at different temperatures T_0.

Table II: Heating parameters.

TABLES

Table I:

T_0 [K]	τ_a [μs]	τ_L [ms]	τ_r [ms]
0.75	3.10	0.15	2.21
1	4.99	0.25	1.99
1.5	10.37	0.53	1.84
2	17.05	0.85	1.79
3	43.03	2.15	1.75

Table II:

	T_0 [K]	$T_1^{\rm est}$ [K]	$T_1^{\rm fit}$ [K]	τ_a [μs]
PMMA	0.75	1.3	1.5	300
	1.5	1.7	1.7	
	3	3	3	
EtOD	1.75	2.55	2.65	15
	2.4	2.8	2.8	
	3	3.3	3.3	

FIGURES

FIG. 1.

FIGURES

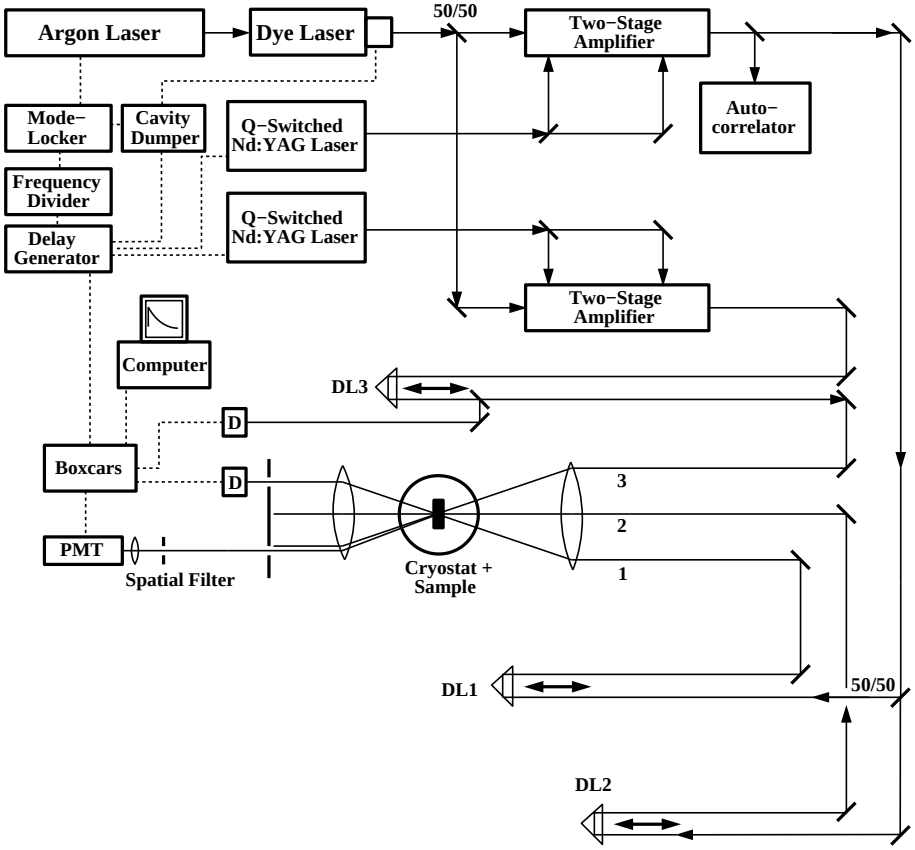
Argon Laser
Dye Laser
50/50
Two−Stage Amplifier
Auto− correlator
Mode− Locker
Cavity Dumper
Q−Switched Nd:YAG Laser
Frequency Divider
Delay Generator
Q−Switched Nd:YAG Laser
Two−Stage Amplifier
Computer
DL3
D
Boxcars
D
3
2
PMT
Spatial Filter
Cryostat + Sample
1
DL1
50/50
DL2

FIG. 2.

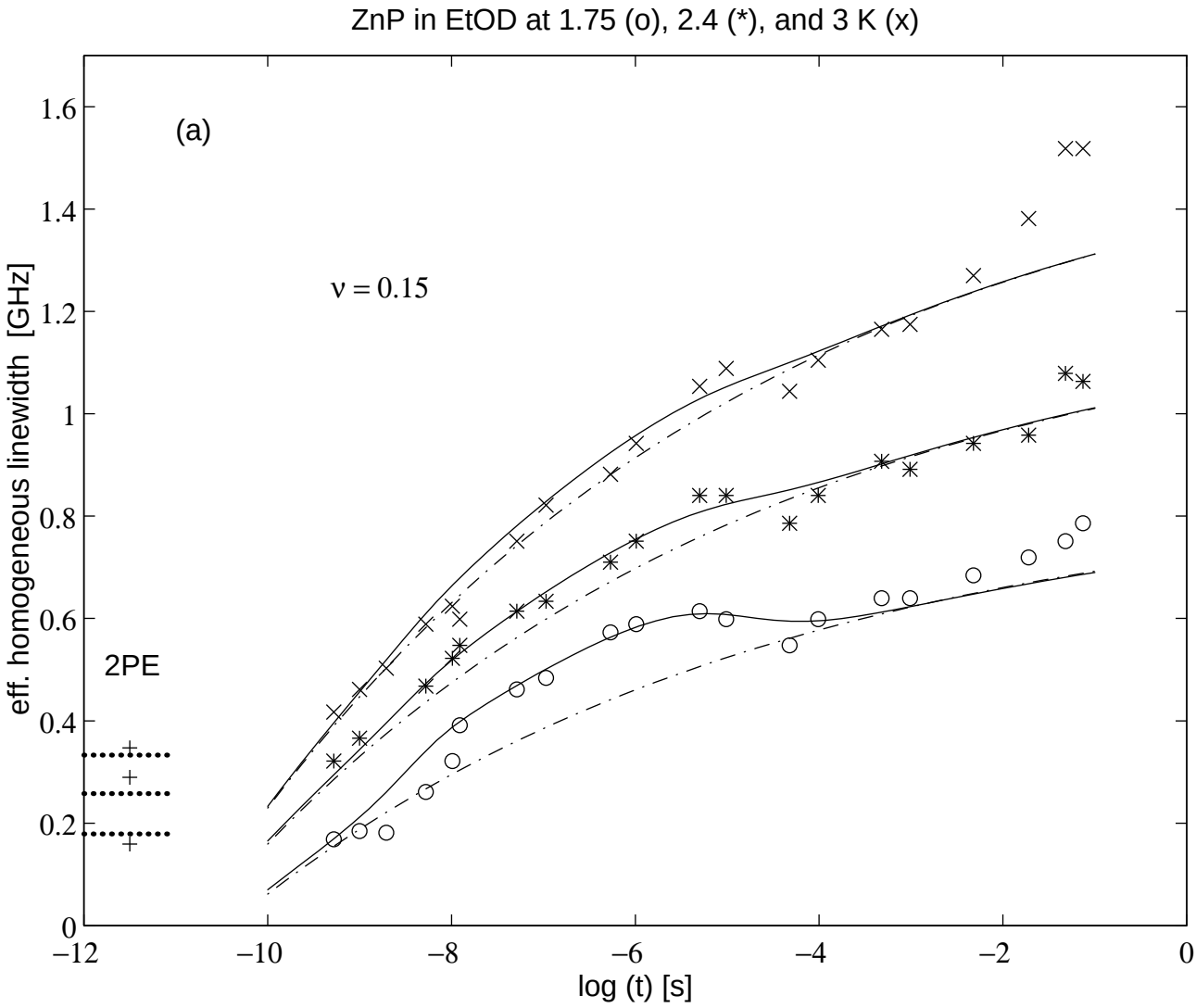
ZnP in EtOD at 1.75 (o), 2.4 (*), and 3 K (x)
(a)
ν = 0.15
2PE
eff. homogeneous linewidth [GHz]
log (t) [s]
0
0.2
0.4
0.6
0.8
1
1.2
1.4
1.6
−12
−10
−8
−6
−4
−2
0

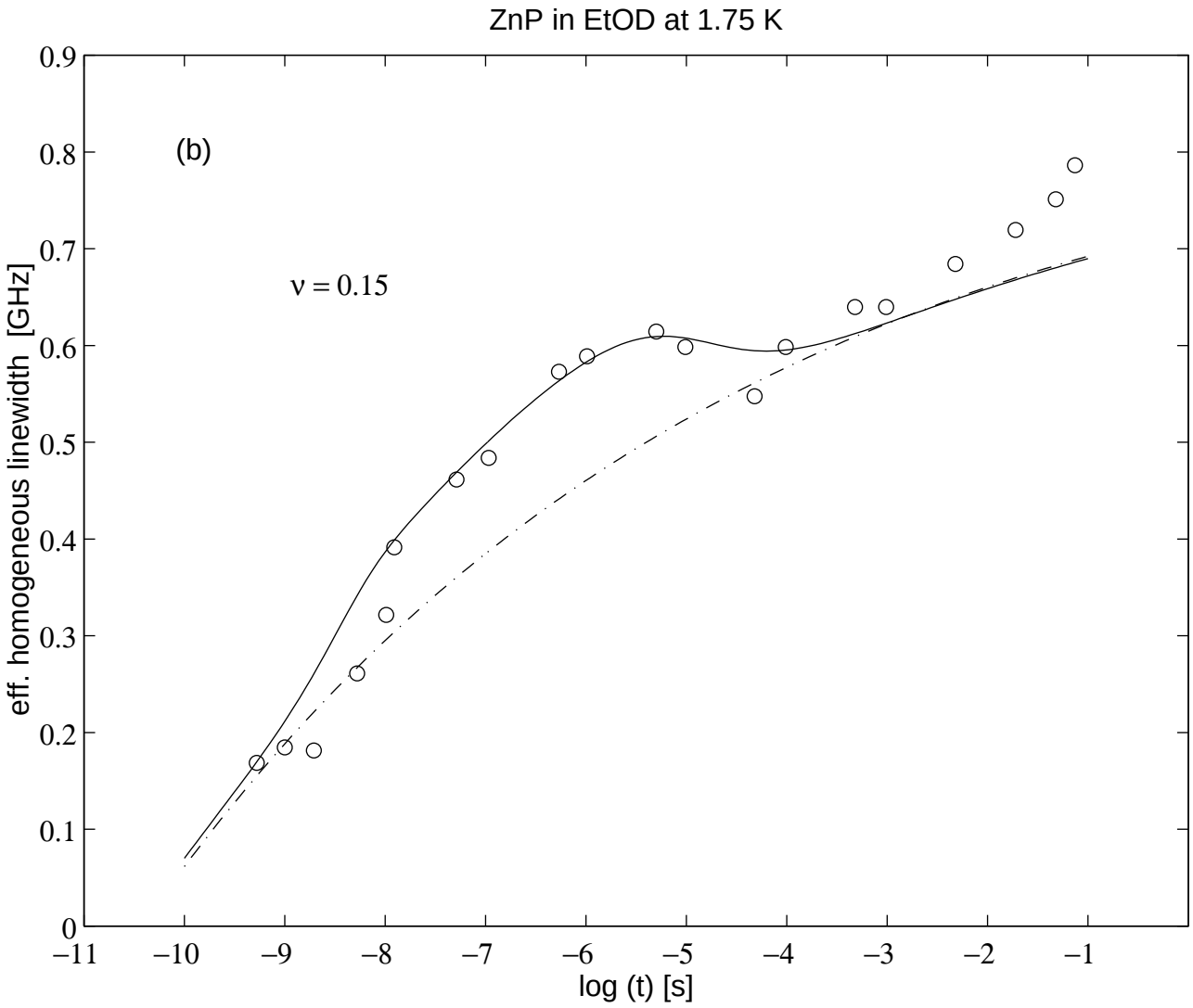
ZnP in EtOD at 1.75 K
(b)
ν = 0.15
eff. homogeneous linewidth [GHz]
log (t) [s]
0.9
0.8
0.7
0.6
0.5
0.4
0.3
0.2
0.1
0
−11
−10
−9
−8
−7
−6
−5
−4
−3
−2
−1

FIG. 3.

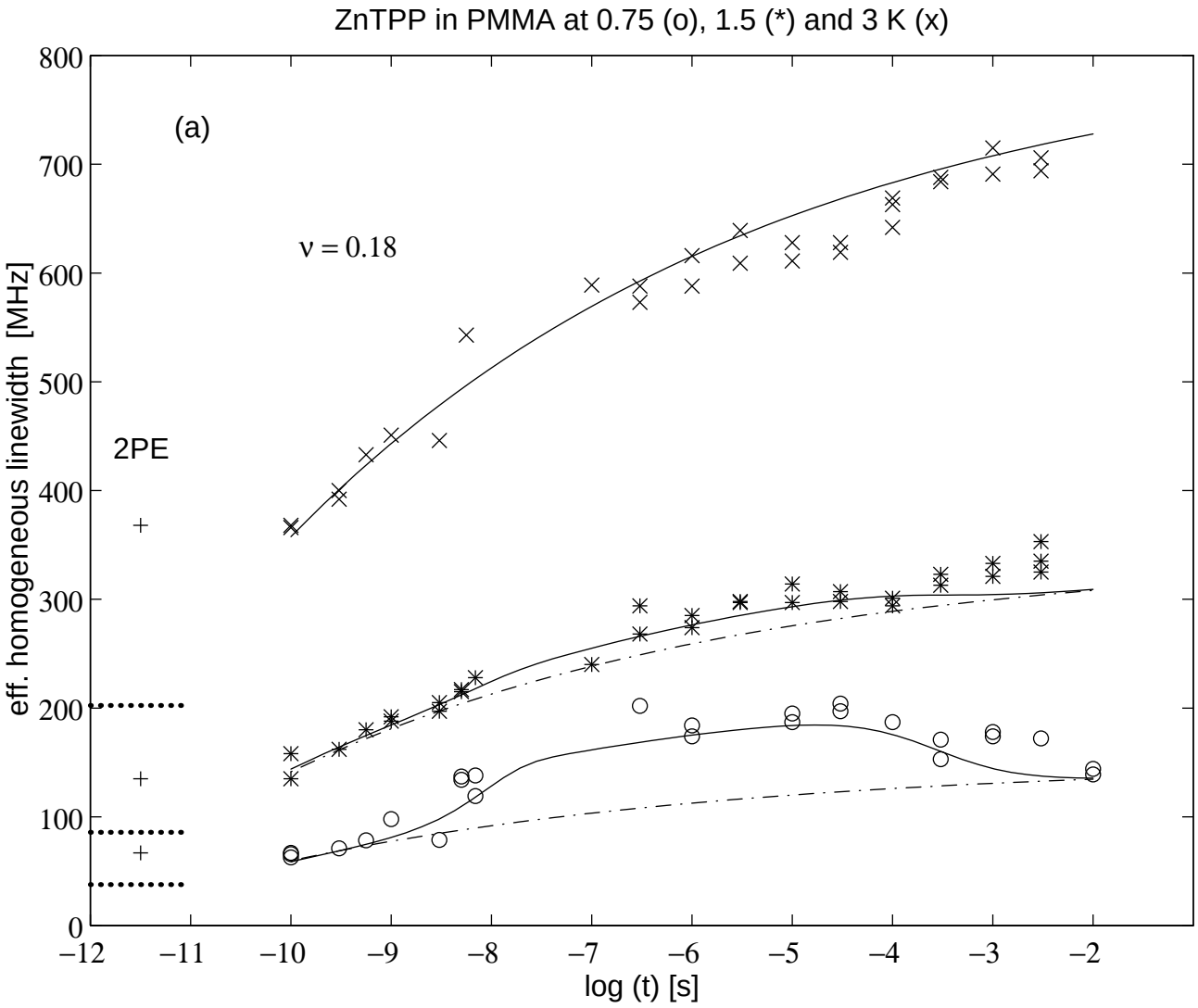
ZnTPP in PMMA at 0.75 (o), 1.5 (*) and 3 K (x)
(a)
ν = 0.18
2PE
eff. homogeneous linewidth [MHz]
log (t) [s]
800
700
600
500
400
300
200
100
0
−12
−11
−10
−9
−8
−7
−6
−5
−4
−3
−2

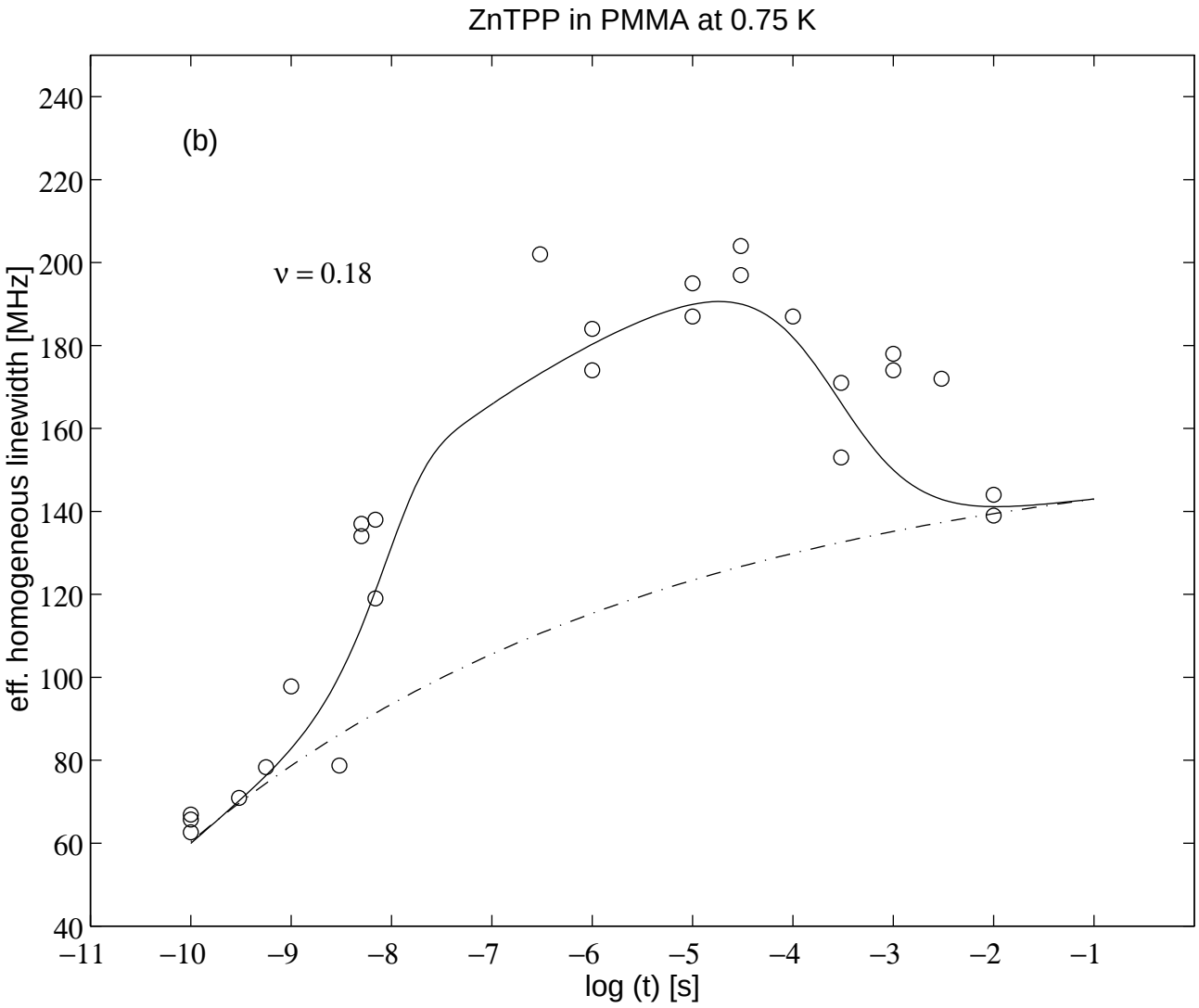
ZnTPP in PMMA at 0.75 K
(b)
ν = 0.18
eff. homogeneous linewidth [MHz]
log (t) [s]
240
220
200
180
160
140
120
100
80
60
40
−11
−10
−9
−8
−7
−6
−5
−4
−3
−2
−1

FIG. 4.

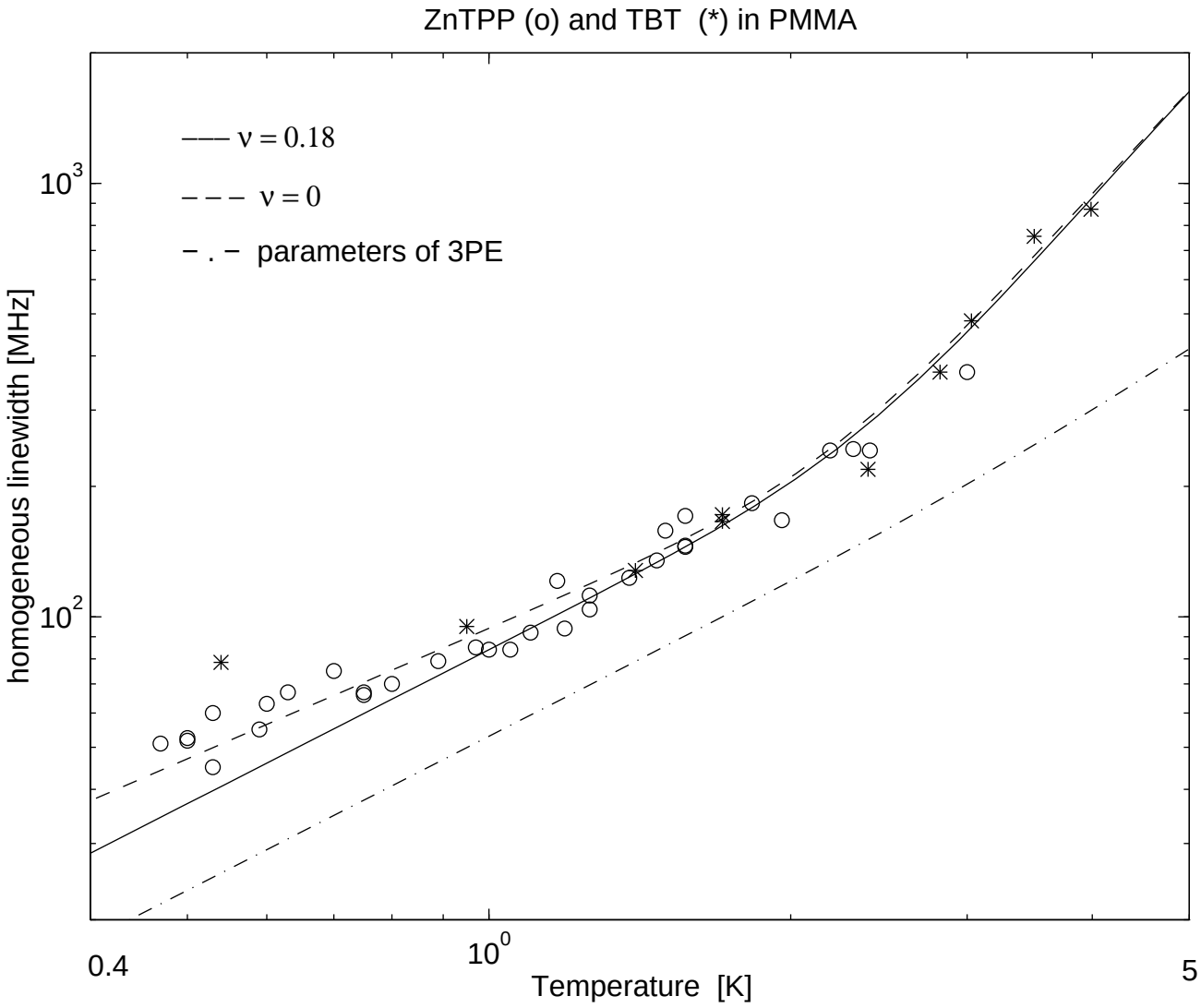
ZnTPP (o) and TBT (*) in PMMA
—— ν = 0.18
– – – ν = 0
– . – parameters of 3PE
homogeneous linewidth [MHz]
10^3
10^2
0.4
10^0
5
Temperature [K]